Petroleum Science 23 (2026) 3634–3646

Contents lists available at ScienceDirect

Petroleum Science

journal homepage: www.keaipublishing.com/en/journals/petroleum-science

Original Paper

Mesoscopic mechanism of shear breakdown and static recovery characteristics of waxy crude oil gel structures

Li-Ping Guo [a,*], Jia-Jun Zhang [a], Lei Wang [b], Rui Chen [c], Bao-Jun Liu [a]

[a] Key Laboratory for Enhanced Oil & Gas Recovery of the Ministry of Education, Northeast Petroleum University, Daqing, 163318, Heilongjiang, China
[b] Exploration and Development Research Institute, Daqing Oil Field Company Ltd., Daqing, 163712, Heilongjiang, China
[c] CNOOC Oilfield Engineering Co., Ltd., Tianjin, 300450, China

A R T I C L E I N F O

Article history:
Received 27 September 2025
Received in revised form
9 December 2025
Accepted 20 January 2026
Available online 25 January 2026

Edited by Meng-Jiao Zhou

Keywords:
Waxy crude oil
Wax crystal morphology
Mesoscopic mechanism
Shearing
Static recovery

A B S T R A C T

The primary method for transporting high-wax crude oil is heated pipeline transmission. During shutdowns, the gelled state and structural strength of the congealed oil directly determine the restart pressure required for pipeline resumption, with wax crystals being the dominant internal factor. This study employs synchronized macro-meso rheological measurements to systematically investigate the continuous evolution of wax crystal morphology during network formation, shear-induced yielding, and static recovery, while analyzing the effects of shear cycles and rate. Results indicate that during the isothermal gelation stage after cooling, continuous precipitation, growth, and aggregation of wax crystals lead to significant changes in mesoscopic characteristic parameters (2.60%–45.17%). In the initial shearing stage, the wax crystal network sequentially undergoes yield deformation, fragmentation, and eventually reaches a dynamic equilibrium state where deformation, fragmentation and reaggregation coexist. With increasing shear cycles, wax crystals experience more thorough fragmentation, developing a denser and more uniform spatial distribution with their shapes tending toward sphericity. During the subsequent static recovery stage, only partial fragmented wax crystals undergo re-adsorption and aggregation, resulting in limited changes in characteristic parameters (0.27%–9.84%). Higher shear rates increase the yield stress and shorten the yielding time, while reducing both the equilibrium stress value and structural parameters, simultaneously exacerbating irreversible damage to the wax crystal network and inhibiting the recovery capability of the gelled structure. This study elucidates the correlation mechanism between mesostructural evolution of wax crystals and macroscopic rheological behavior during shear-recovery processes, providing theoretical foundations for addressing complex engineering challenges in pipeline restart operations.

1. Introduction

Petroleum remains one of the world's primary fossil energy sources (Li et al., 2022), with high-wax crude oil—characterized by its high pour point and viscosity—accounting for over 80% of China's total crude production (Wang et al., 2023). Consequently, heated pipeline transportation has become the predominant method for oil delivery in cold regions. Pipeline shutdowns are inevitable due to accidents or planned maintenance. During low-temperature shutdowns, the cessation of shear forces allows dispersed wax crystals in the crude oil to flocculate and grow, forming gelled crude oil with a certain structural strength (Yao et al., 2023), which exhibits complex rheological behavior. The presence of wax crystals (including individual crystals and their aggregates) is the primary factor contributing to the low-temperature gelling of crude oil (Kiyingi et al., 2023; Mohammadi and Mahmoudi, 2021).Current research on the rheological properties of gelled waxy crude oil predominantly relies on macro-rheological measurements, lacking in-depth mechanistic understanding at the mesoscopic level. Investigating the continuous evolution of wax crystal morphology during the formation, shear-induced yielding and breakdown, and isothermal static recovery processes of gelled crude oil structures serves as an effective approach to study the structural breakdown and recovery characteristics from a mesoscopic perspective.

* Corresponding author.
E-mail address: glp_dqsy@sina.com (L.-P. Guo).
Peer review under the responsibility of China University of Petroleum (Beijing).

https://doi.org/10.1016/j.petsci.2026.01.035
1995-8226/

Currently, among the techniques for observing wax crystal characteristics, optical microscopy has gained widespread application due to its ability to directly capture the morphology and structure of wax crystals. Letoffe et al. (1995) demonstrated through optical microscopy that wax crystal size depends on the carbon chain length of paraffin, typically ranging between 1 and 3 μm. Henaut et al. (1999) conducted observations of wax crystallization using polarized light microscopy. The results indicated that wax crystals exhibit a lamellar structure, where individual layers overlap and interlock to form a crystalline framework. Liquid hydrocarbons become trapped within this framework, ultimately developing a gelled structure. Srivastava et al. (2002) utilized phase-contrast microscopy to investigate the crystallization process of waxy crude oil, identifying two distinct crystal forms: rod-like and plate-like structures.

The development of digital image processing has enabled researchers to shift from subjective wax crystal comparisons to objective quantitative evaluations. Shuang et al. (2002) developed an analytical framework incorporating mathematical morphology principles and an enhanced circularity detection algorithm to quantify microstructural characteristics like crystal size parameters, shape factors, and liquid-phase configuration. The analytical results provided measurable parameters such as crystal sphericity, size distribution patterns, and developmental zone features, establishing a comprehensive methodology for quantifying wax crystalline architectures and microstructural configurations. Blake and Marangoni (2015) utilized pore area fraction as a metric for quantifying wax crystal coverage area. Zhao et al. (2021) adopted four key parameters—crystal number, area, aspect ratio, and fractal dimension—as mesostructural descriptors for wax crystal morphology. Additionally, he characterized crystal aggregation and orientation by measuring inter-crystal centroid distances and the angular deviation between crystal major axes and shear flow direction.

Building upon these quantitative methods, researchers have investigated wax crystal structural evolution under shear. Venkatesan et al. (2005), using a synchronized rheo-optical measurement system, demonstrated that shear during cooling significantly alters crystal morphology. At low shear rates, pronounced crystal flocculation occurred with accelerated network formation, whereas high shear rates caused structural fragmentation, preventing complete flocculation and substantially reducing crystal size. Zhao et al. (2021) conducted microscopic studies revealing distinct shear effects during the cooling stage of waxy crude oil, where low shear promotes wax aggregation, moderate shear simultaneously induces aggregation and dispersion, while high shear primarily causes dispersion. Complementing these findings, Dong et al. (2022) observed through microscopic experiments that increasing shear rates transition isothermally sheared waxy crude oil from static to dynamic states, with the gel network progressively undergoing deformation, disintegration, and eventual breakdown into smaller flow-aligned clusters that continue deforming under sustained shear. Wang et al. (2020) employed fractal dimension analysis to interpret shear-dependent aggregation behavior, discovering enhanced crystal clustering at reduced shear effects. Higher shear rates corresponded to lower fractal dimensions, indicating weakened nonlinear structural features in crystal aggregates.

Regarding the structural recovery properties of gelled waxy crude oil, Li and Lu (2004) employed an RS75 rheometer to investigate non-Newtonian crude oil using small-amplitude oscillatory shear measurements. The study revealed that non-Newtonian crude oil constitutes a strongly flocculated system with irreversible thixotropic behavior, where higher pre-shear intensities lead to lower static structural recovery levels. Hou and Zhang (2005) conducted oscillatory shear experiments on Daqing crude oil using an RSH150 controlled-stress rheometer. The study revealed that the structural recovery of the crude oil after shear deformation exhibited irreversible characteristics. Lin et al. (2009) conducted theoretical derivation and rheological experiments to study the isothermal gelation process of thixotropic waxy crude oil. The results showed that the structural strength developed during isothermal static conditions weakened with increasing temperature, higher preshear rates, and prolonged preshear time. Research by Jia and Zhang (2012) revealed that maintaining waxy crude oil at pour point temperature induces time-dependent structural changes: gel structural strength and yield stress progressively increase, while structural reversibility concurrently decreases. This reduced reversibility indicates structural damage becomes increasingly irreversible, rendering restoration to the original state more difficult following disruption. Bao et al. (2016) examined structural evolution in waxy crude oil under both isothermal and cooling conditions after pre-shearing using a rheometer. Their findings indicated that once the gelled structure is disrupted, neither isothermal static holding nor further cooling can fully restore the strength achieved under static cooling conditions.

In summary, while previous studies have utilized optical microscopy to examine wax crystal morphology and its evolution under shear in crude oil, most investigations have focused on specific conditional effects without systematically characterizing the entire process of structural formation, shear-induced yielding, and isothermal static recovery in gelled crude oil. The study employs *in situ* microscopic observation technology to monitor the mesoscale morphological evolution of wax crystals throughout multiple cycles of structural formation, shear loading, and isothermal static recovery, analyzing both the continuous morphological changes and spatial distribution characteristics of wax crystals. By correlating these observations with synchronous macro-rheological test data, the research systematically investigates the effects of shear cycles and shear rates. The findings elucidate the mesoscale mechanisms underlying the structural breakdown and recovery of gelled waxy crude oil, b while establishing theoretical foundations for solving practical pipeline restart challenges. The study bridges the gap between microscale structural evolution and macroscopic flow behavior, advancing both fundamental understanding and practical applications in waxy crude oil transportation.

2. Experimental section

2.1. Materials

In this study, Daqing crude oil was selected as a typical waxy crude. Table 1 summarizes its key physical properties along with the respective testing methods.

Prior to testing, the oil samples must undergo thermal pretreatment to eliminate their "memory effect" (Guo et al., 2022) and ensure rheological reproducibility. The standardized procedure consists of: (1) homogenizing the crude oil by mechanical agitation before aliquoting into 100 mL amber glass bottles with ground-in stoppers to maintain compositional consistency; (2) thermally equilibrating the samples in an 80 °C water bath for 2 h to achieve molecular-level uniformity through Brownian motion; (3) subsequent storage in a light-proof incubator at constant temperature for a minimum 48-h stabilization period before experimentation.

2.2. Apparatus

The mesoscopic experiments employed HAAKE MARS III rheometer's RheoScope module (Germany), featuring integrated optical microscopy, precise temperature regulation, and digital imaging capabilities (Fig. 1). The imaging system comprised a 10 × ocular lens and 20 × objective lens, providing 200 × magnification. Shear deformation was applied using a polished 60 mm diameter cone-plate geometry, the sample thickness was 52 μm. Temperature stability (±0.01 °C) was maintained throughout testing using a Haake A25 recirculating bath.

2.3. Experimental steps and analysis methods

The pretreated oil samples were transferred from the incubator to a programmable water bath maintained at 60 °C for 30 min before being placed on the preheated rheometer microscope stage at the same temperature. Following sample loading, the system was held isothermally for 5 min to achieve thermal equilibrium, after which controlled cooling was initiated at a rate of 0.5 °C/min until reaching the target temperature of 34 °C. At this temperature, the samples underwent a 40-min isothermal stabilization period to ensure complete development of the waxy crude oil's gelled structure. Subsequently, shear loading tests were conducted sequentially at rates of 0.3, 0.5, 0.8, and 1.0 s^{-1}, each maintained for 10 min. To investigate structural recovery characteristics, after the initial shearing cycle, the samples were allowed to recover under isothermal conditions for 30 min before applying identical secondary shear loading. Following these first two shear cycles, an extended 60-min recovery period preceded the third shear application, maintaining consistent shear parameters with the previous cycles. Throughout the entire experimental process—from initial cooling through final shearing —microscopic image acquisition was systematically performed: during cooling, five images were captured per 1 °C temperature decrement; isothermal stages required one image every 30 s; while shear loading stages demanded higher temporal resolution with one image per second (Zhao et al., 2021). To guarantee experimental reproducibility and result reliability, all tests were performed in triplicate under identical conditions.

2.4. Micrograph analysis and quantification techniques

The wax crystal microscopic images underwent a three-stage processing procedure using ImageJ software: format conversion, threshold segmentation, and parameter extraction. Initially, the original RGB images were converted into 8-bit grayscale images, with fixed contrast optimization (91–251) applied to enhance the wax crystal boundaries in 90% of the images significantly. Subsequently, a comparative test of sixteen global threshold algorithms conducted on thirty thousand wax crystal images revealed that the Intermodes threshold algorithm performed optimally within the 4%–5% threshold range, enabling clear identification of wax crystal contours in over 95% of the images. Consequently, this method was adopted for processing the microscopic images in this study, as exemplified by the conversion from Fig. 2(a) to Fig. 2(b). Following threshold processing, the wax crystal particle contour map (Fig. 2(c)) and triangulation diagram (Fig. 2(d)) were extracted to calculate geometric parameters. Additionally, the box-counting method was employed to quantify the fractal dimension ($1 < D < 2$) of wax crystal aggregates. This approach, utilizing multi-scale grid coverage and logarithmic regression analysis, effectively characterized the structural complexity of wax crystals.

Table 1
Physical properties of the Daqing crude oil.

Parameter	Value	Test method
Pour point, °C	36	ASTM D5853-11
Density at 20 °C, kg/m^3	865.54	ISO 3675-1998
Viscosity at 50 °C, mPa·s	25.95	ASTM D4287-2000
Wax appearance temperature, °C	49.98	ASTM D4419-90
Wax content, wt%	23.56	
Saturates content, wt%	81.2	ASTM D4124-09
Aromatics content, wt%	16.1	
Resin content, wt%	0.4	
nC_7-Asphaltene content, wt%	2.3	
<C_{17}, wt%	19.53	ASTM D7169-18
C_{17}–C_{35},wt%	29.94	
C_{36}–C_{55}, wt%	9.24	
C_{56}–C_{94}, wt%	11	

3. Results and discussions

3.1. Mesoscopic mechanism of structural formation and recovery in gelled waxy crude oil

The rheological properties of waxy crude oil exhibit distinct temperature-dependent characteristics. At elevated temperatures, wax components exist in liquid hydrocarbon form, rendering the crude oil a single-phase Newtonian fluid. When cooled below the wax precipitation temperature, wax crystals gradually precipitate to form a liquid-solid biphasic system. Further temperature reduction triggers three-dimensional network structure formation through wax crystal interconnections, transforming the system into a gelled state (Sun et al., 2019). This gelled structure demonstrates characteristic thixotropy—when disrupted by shear forces, the dispersed wax particles undergo reassociation and coalescence during subsequent isothermal static conditions (Zhao et al., 2024), progressively reconstructing the damaged network into a new spatial configuration. Notably, the restored gel strength exhibits positive correlation with resting duration, a phenomenon termed the static recovery characteristic of gelled waxy crude oil. To thoroughly investigate the mesoscopic mechanism of gelled structure formation and isothermal static recovery characteristics in waxy crude oil, the wax crystal micrographs at different isothermal static stages during experiments were analyzed. The isothermal process was divided into three stages: the first stage represents the gelation stage of waxy crude oil after cooling (initial structure formation), the second stage corresponds to the structural recovery stage after initial shearing, and the third-stage involves the structural re-recovery stage following secondary shearing. Each stage employed integrated macro-rheological testing with *in situ* polarized light microscopy to achieve real-time correlation analysis between mesostructural morphology and macroscopic rheological parameters.

Taking the experiment with a heating temperature of 60 °C, cooling rate of 0.5 °C/min, and shear rate of 0.3 s^{-1} as an example, wax crystal micrographs at different isothermal stages and time points were compiled for comparative analysis, as shown in Fig. 3. Each row of wax crystal micrographs represents images at different isothermal time points within the same isothermal stage. With prolonged isothermal duration, wax crystals progressively precipitated and grew.

To compare the precipitation and growth of wax crystals across the three stages, this study superimposed wax crystal images taken at the beginning (0 min) and after 30 min of isothermal conditions for each stage, as shown in Fig. 4. In the figure, the gray areas represent overlapping wax crystal structures before and after the isothermal period, while the black areas indicate newly precipitated and grown wax crystals after 30 min. Comparative analysis revealed that the first isothermal stage exhibited the most significant wax crystal precipitation and growth, followed by the second stage, with the third stage showing the least development.

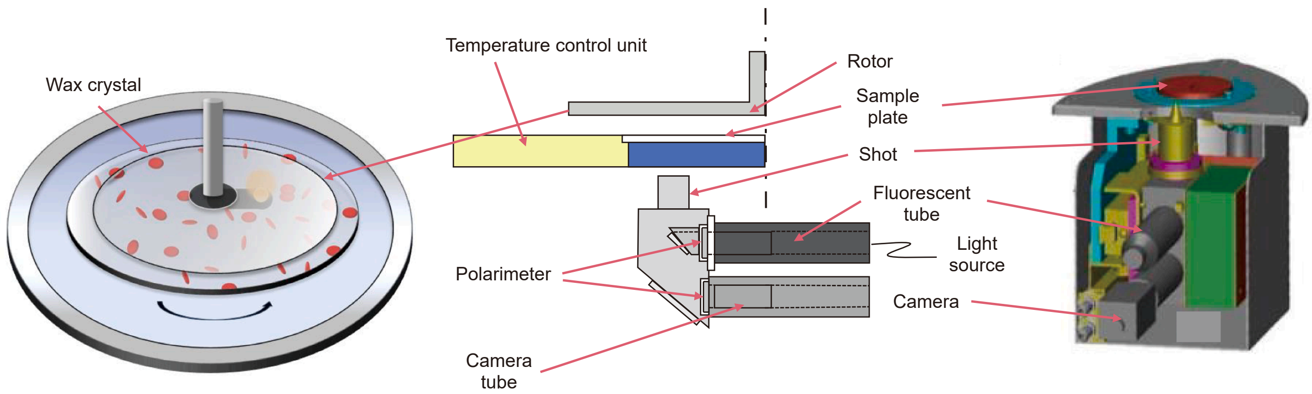

Fig. 1. Diagram of experimental equipment.

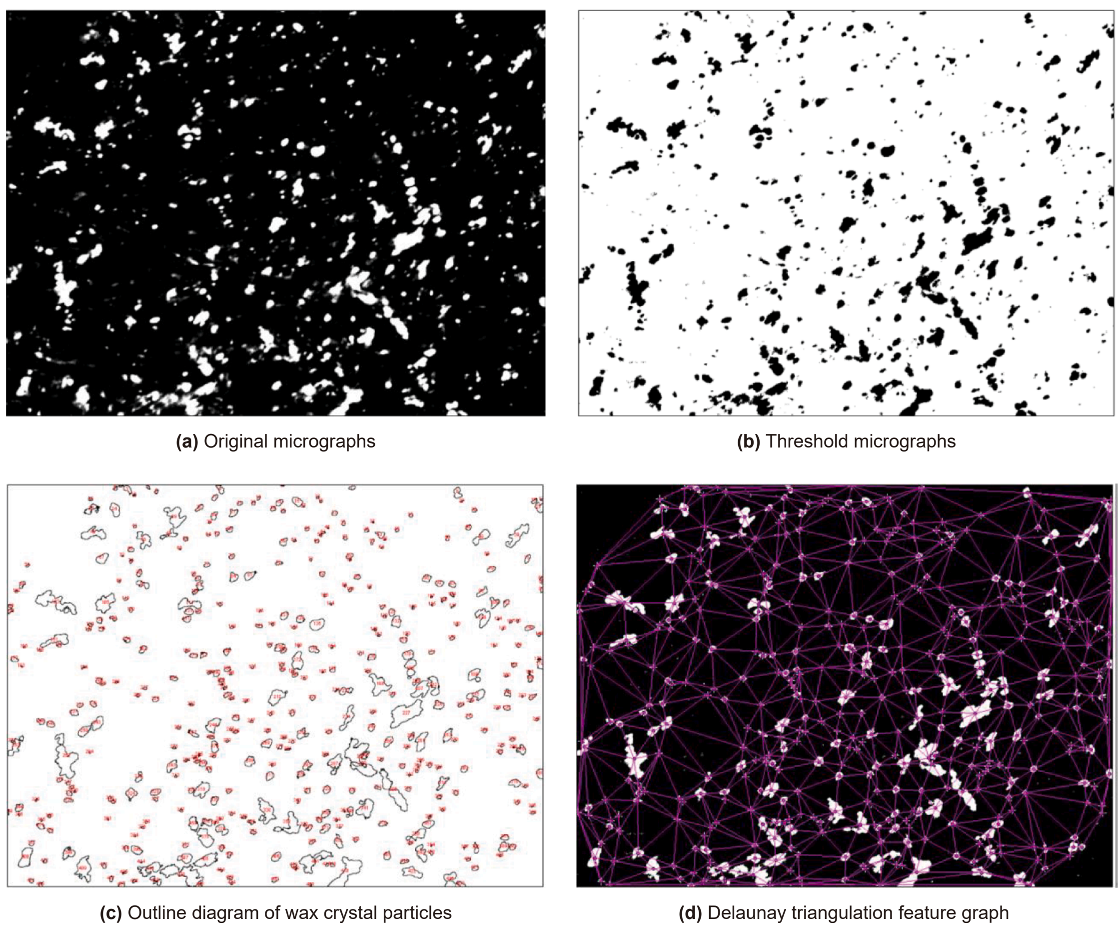

Fig. 2. Wax crystal image processing and quantitative identification process.

To quantitatively analyze the gelation structure formation and recovery characteristics of waxy crude oil from a mesoscopic perspective, this study processed wax crystal images from different isothermal stages using ImageJ software. Key mesoscopic parameters including crystal number, area, fractal dimension, and aspect ratio were extracted as shown in Fig. 5. As a morphological parameter, the aspect ratio demonstrates greater values for rod-like crystals compared to spherical particles. The fractal dimension quantifies structural complexity, with greater values corresponding to more intricate spatial distributions and network configurations of wax crystals (Zhao et al., 2021).

Fig. 5 demonstrates that during the first 10 min of the initial isothermal stage after cooling, the mesoscopic parameters of wax crystals exhibited the most significant changes. This phenomenon occurs because the crude oil's wax had not completely precipitated at this stage, allowing substantial dissolved wax to continuously crystallize and grow, leading to considerable increases in crystal number, area, and fractal dimension (3.19%–25.51%). Concurrently, newly formed wax crystals aggregated under Brownian motion and van der Waals forces, forming more compact clusters and causing a substantial decrease in average aspect ratio (4.29%) (Dong et al., 2020). As the process transitioned from wax

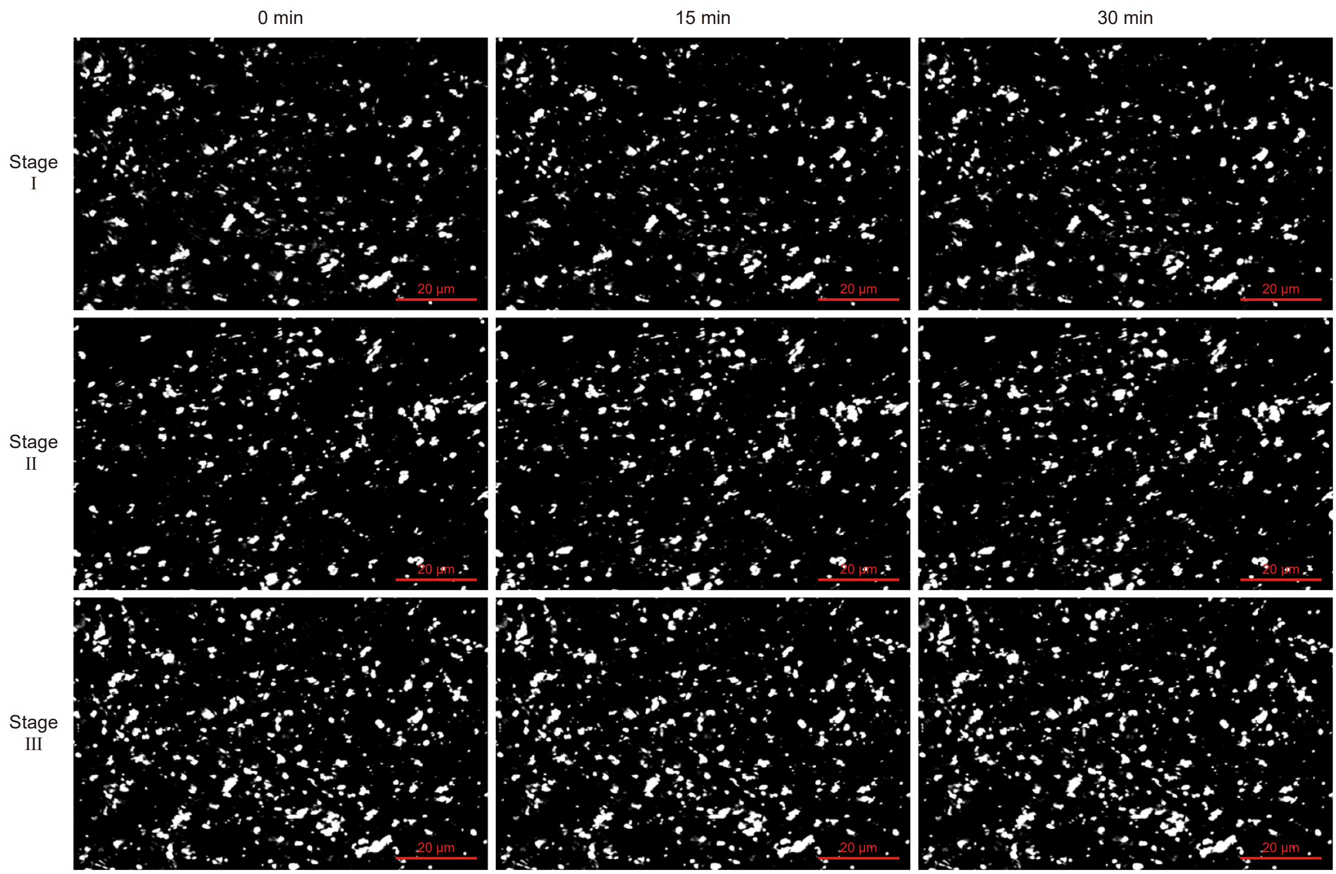

Fig. 3. Wax crystal micrographs at different time points during isothermal stages. Conditions: heating temperature 60 °C; cooling rate 0.5 °C/min.

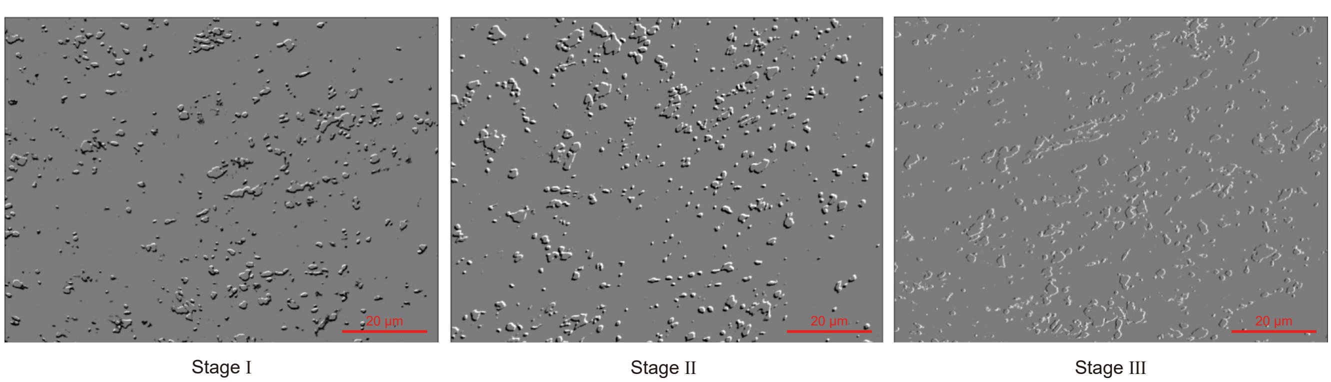

Fig. 4. Superimposed wax crystal images before and after isothermal treatment at different stages. Conditions: heating temperature 60 °C; cooling rate 0.5 °C/min.

precipitation to crystal growth and coalescence, the mesoscopic parameters changed more gradually (0.07%–2.93%), marking the formation of the gelation structure. In the later isothermal phase, the average aspect ratio slowly increased as the system stabilized, with the anisotropic growth characteristics of wax molecules becoming dominant—their chain-like structure promoted crystal growth along the molecular chain direction (long axis), thereby increasing the aspect ratio. In contrast, the second and third isothermal stages following shear treatment showed smaller variations in mesoscopic parameters. This is because the gelled structure of waxy crude oil, after undergoing shear, experienced minimal new wax precipitation. Instead, only fragmented wax crystals damaged during shearing re-adsorbed and re-aggregation onto existing crystals, resulting in smaller changes in mesoscopic characteristics (0.27%–11.1%). The aspect ratio and fractal dimension both demonstrated excellent repeatability, with SD ranges of 0.015–0.14 and 0.005–0.11, and CVs of 0.86%–7.89% and 0.32%–9.24%, respectively.

The spatial distribution characteristics of wax crystals are a critical factor influencing the structural strength of crude oil. In this study, we employed Delaunay triangulation to quantitatively analyze wax crystal images. The methodology begins with image processing to extract the coordinates of wax crystal centers, followed by the construction of Delaunay triangular meshes. This

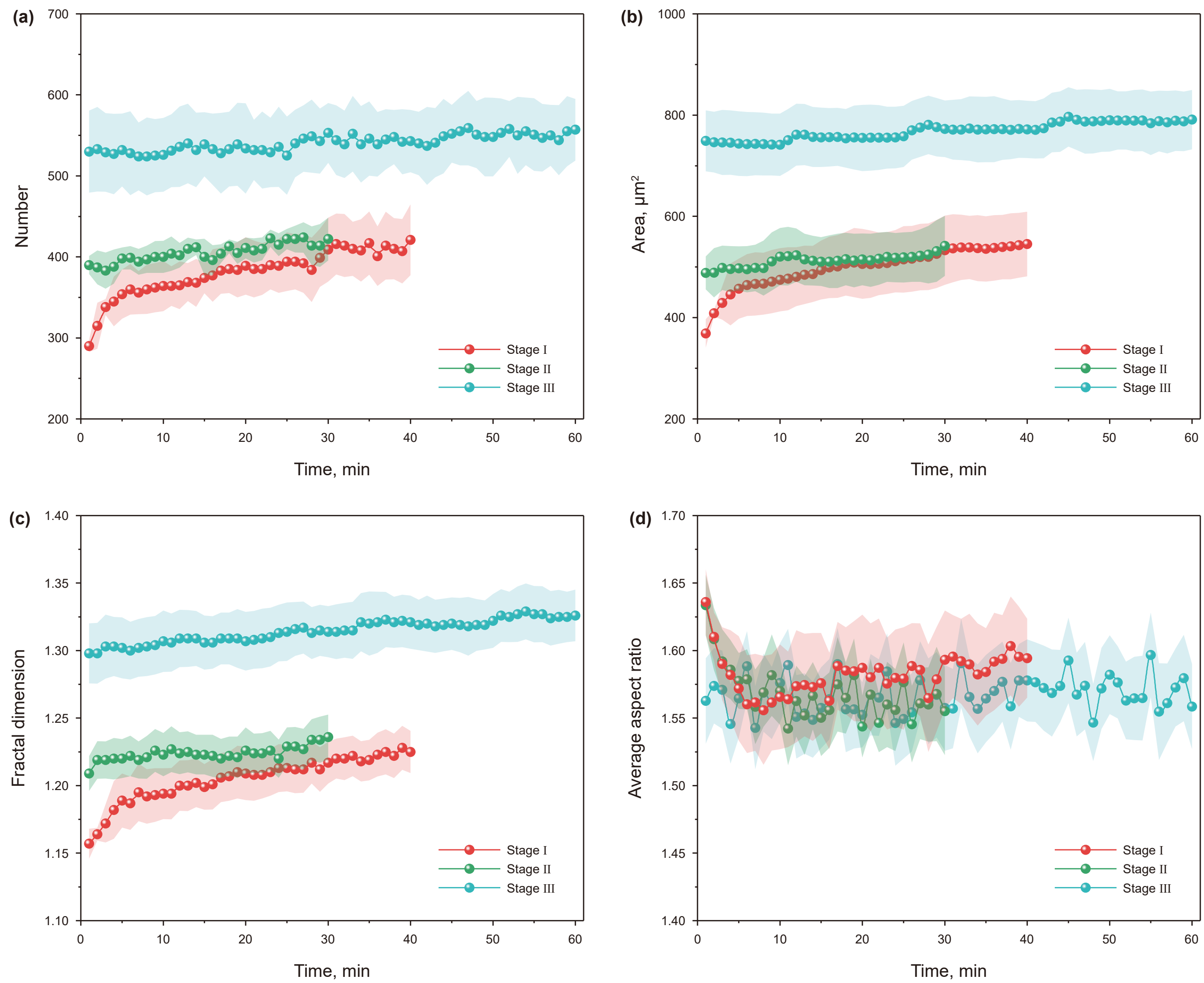

Fig. 5. Variation of mesoscopic characteristics of wax crystals with isothermal time at different stages. **(a)** Wax crystal number; **(b)** wax crystal area; **(c)** wax crystal fractal dimension; **(d)** wax crystal average aspect ratio. Conditions: heating temperature 60 °C; cooling rate 0.5 °C/min.

approach automatically connects adjacent crystals to form an optimized triangular network. Based on the triangulation results, two key parameters were calculated: The average wax crystal spacing, obtained by statistically analyzing the mean edge lengths of all triangles, reflects the overall distribution density. Meanwhile, the variance of nearest-neighbor distances characterizes local uniformity, determined by measuring the dispersion of distances from each crystal to its closest neighbor. A smaller variance indicates more homogeneous spatial distribution of wax particles.

The temporal variations of average wax crystal spacing and nearest-neighbor distance variance during different isothermal stages of waxy crude oil are presented in Fig. 6. As shown in Fig. 6(a), the average wax crystal spacing gradually decreases with prolonged isothermal time across all stages, indicating enhanced spatial distribution density and progressive formation/recovery of the wax crystal network. Notably, the first isothermal stage demonstrates more significant improvement than subsequent stages. This phenomenon occurs because substantial dissolved wax continues to precipitate and grow during the initial stage, leading to considerable increase in crystal number. In contrast, the second and third stages following shear treatment exhibit minimal new crystal formation, with only fragmented crystals from shear-induced damage re-aggregating onto existing structures, resulting in slower growth rates. Furthermore, Fig. 6(a) reveals that progressive isothermal stages yield reduced average spacing, reflecting increased spatial density. This trend emerges because repeated shear treatments promote further crystal fragmentation, thereby increasing crystal number and distribution density. Correspondingly, Fig. 6(b) demonstrates decreasing variance of nearest-neighbor distances over time, confirming improved spatial uniformity across all stages. These parallel trends in both parameters establish that extended isothermal duration and advanced processing stages simultaneously enhance both the density and homogeneity of wax crystal distribution.

3.2. Mesoscopic mechanisms of structural breakdown characteristics in gelled waxy crude oil

To investigate the mesoscopic mechanisms of structural breakdown in gelled waxy crude oil under low-temperature conditions, we conducted statistical analysis on micrographs of the gelled structure at different shearing stages (including initial shearing, post-recovery shearing, etc.) under constant temperature. The shearing process was divided into three stages: the first

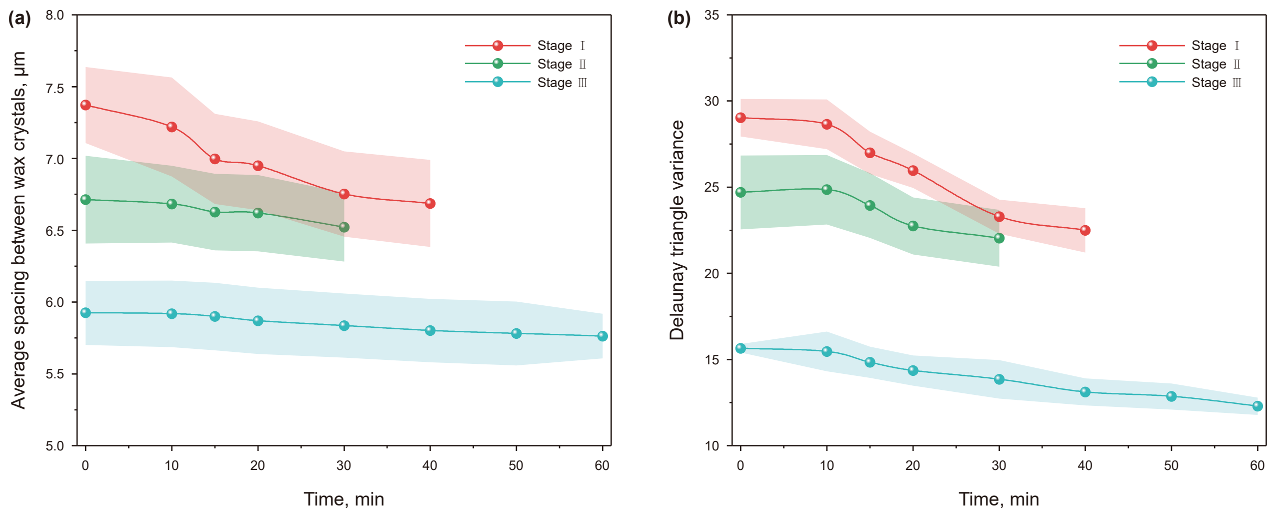

Fig. 6. Temporal variations of average wax crystal spacing and nearest-neighbor distance variance during different isothermal stages. **(a)** Average wax crystal spacing; **(b)** nearest-neighbor distance variance.

stage involved the initial shearing of the waxy crude oil after gelation during cooling; the second stage consisted of re-shearing after the first shearing and subsequent isothermal recovery; the third stage represented the final shearing after the gel structure underwent another isothermal recovery following the previous two shearings.

Taking the experiment with a heating temperature of 60 °C, a cooling rate of 0.5 °C/min, and a shear rate of 0.3 s^{-1} as an example, we performed a comparative analysis by combining micrographs of the waxy crude oil at 3 s before yielding, at yielding, and 1 s after yielding across different shearing stages, as shown in Fig. 7. At 3 s and 2 s before yielding, the gelled system was in a viscoelastic creep stage, exhibiting minor deformation of the wax crystal network. At 1 s before yielding, the system entered a rapid pre-yield deformation stage, where the wax crystal structure underwent significant distortion within a short period. Upon yielding initiation, the wax crystal network began fracturing and disintegrating, accompanied by crystal deformation and re-aggregation (Dong et al., 2022). Horizontal comparison revealed that under identical shearing conditions, the first shearing stage induced the most severe structural fracturing and spatial rearrangement of the 3D wax crystal network during yielding, with more pronounced morphological and spatial distribution changes compared to the second and third shearing stages. Vertical comparison demonstrated that the spatial distribution of wax crystals varied across different shearing stages—with increasing shearing cycles, the wax crystals within the gelled crude oil underwent progressive fragmentation, resulting in a denser and more uniform dispersion.

Comparative analysis of gelled crude oil's macroscopic rheological properties and mesoscopic wax crystal characteristics was conducted to investigate the mesoscopic mechanisms underlying structural breakdown and recovery. The Houska rheological model offers a robust mathematical approach for describing the thixotropic behavior of waxy crude oils and comparable yield-stress fluids. This model demonstrates particular utility due to its dual merits: clear physical representation of thixotropic effects and simultaneous consideration of both yield stress attenuation and consistency degradation processes under shear conditions. Central to this model is the dimensionless structural parameter λ ($0 \le \lambda \le 1$), which quantitatively describes the degree of wax crystal network organization—with $\lambda = 1$ corresponding to maximum structural integrity and $\lambda = 0$ representing total structural collapse (Teng and Zhang, 2013), as mathematically defined in Eq. (1).

$$\begin{cases} \dfrac{\mathrm{d}\lambda}{\mathrm{d}t} = a(1-\lambda) - b\dot{\gamma}^m\lambda \\ \tau = \tau_{y0} + \tau_{y1}\lambda + (k + \Delta k\lambda)\dot{\gamma}^n \end{cases} \tag{1}$$

The model parameters include: τ_{y0} for complete-structure yield stress, Pa, and τ_{y1} for thixotropic yield stress, Pa. Structural kinetics are governed by regeneration rate a, s^{-1}, and degradation rate b, s^{m-1}, supplemented by rheological coefficients k and Δk, Pa·s^n, plus dimensionless exponents m and n. Fig. 8 presents the temporal evolution of shear stress and the structural parameter λ derived from fitting macroscopic experimental data using Eq. (1) under a shear rate of 0.3 s^{-1} across different shearing stages. At the initial stage of shearing, the gelled system undergoes creep, during which the shear stress increases rapidly until reaching the yield point, after which it sharply declines to a stable value (Guo et al., 2015). Experimental results demonstrate significant variations in gelled waxy crude oil across different shear stages: The first stage exhibits the longest shear yield time, highest yield stress, maximum equilibrium shear stress, and peak structural parameters, indicating the most complete wax crystal network structure with optimal strength. In the second stage (after first shear recovery), although structural parameters show partial recovery, they remain substantially inferior to the pristine first stage values. The third stage (after secondary shear recovery) displays further parameter deterioration. This phenomenon stems from the incomplete recovery characteristics of damaged wax crystal networks: Shear forces disrupt the three-dimensional wax crystal structure. While subsequent static rest enables wax crystal reaggregation through van der Waals forces, the high viscosity of the crude oil system severely limits aggregation kinetics. Coupled with accumulated structural defects from repeated shearing, the recovered network consistently fails to achieve the structural integrity of the initial static-cooling-formed configuration (Bao et al., 2016). Moreover, as evident from Fig. 5(b), the wax crystal area in the third stage substantially exceeds that in the first stage. This observation contradicts the conclusion in Reference (Cheng et al., 2000), which posits that larger wax crystal areas correlate with greater structural strength in crude oil. The discrepancy stems from differing

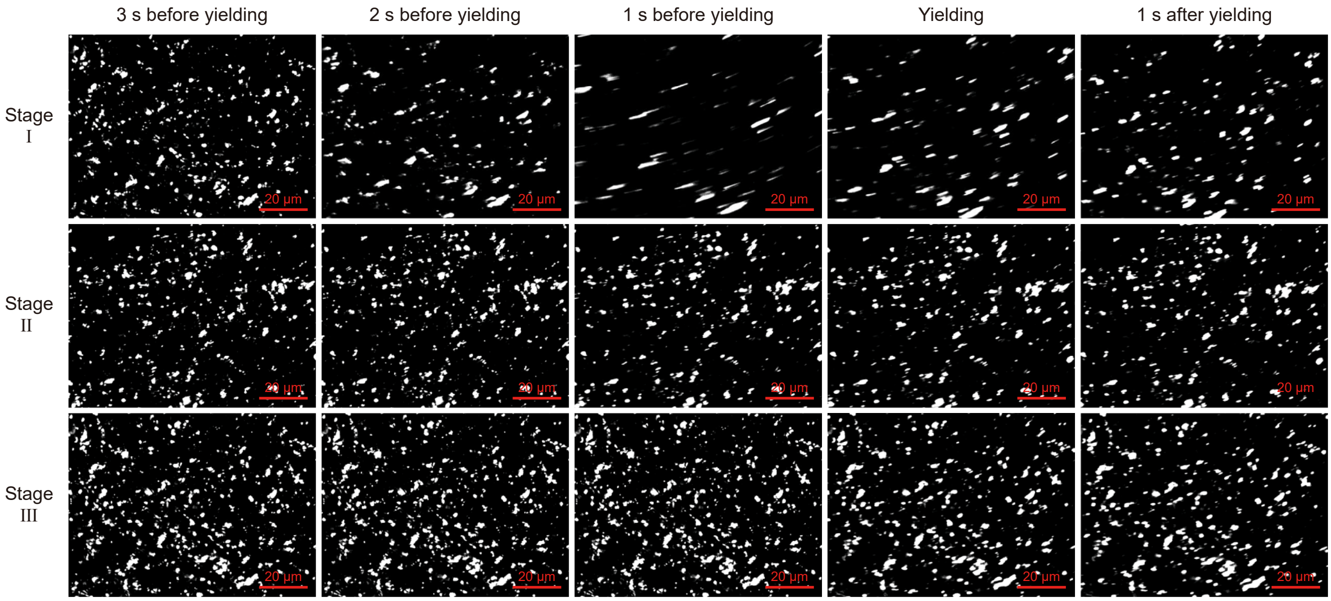

Fig. 7. Evolution images of wax crystals during different shearing stages at 0.3 s^{-1}. Conditions: heating temperature 60 °C; cooling rate 0.5 °C/min; shear rate 0.3 s^{-1}.

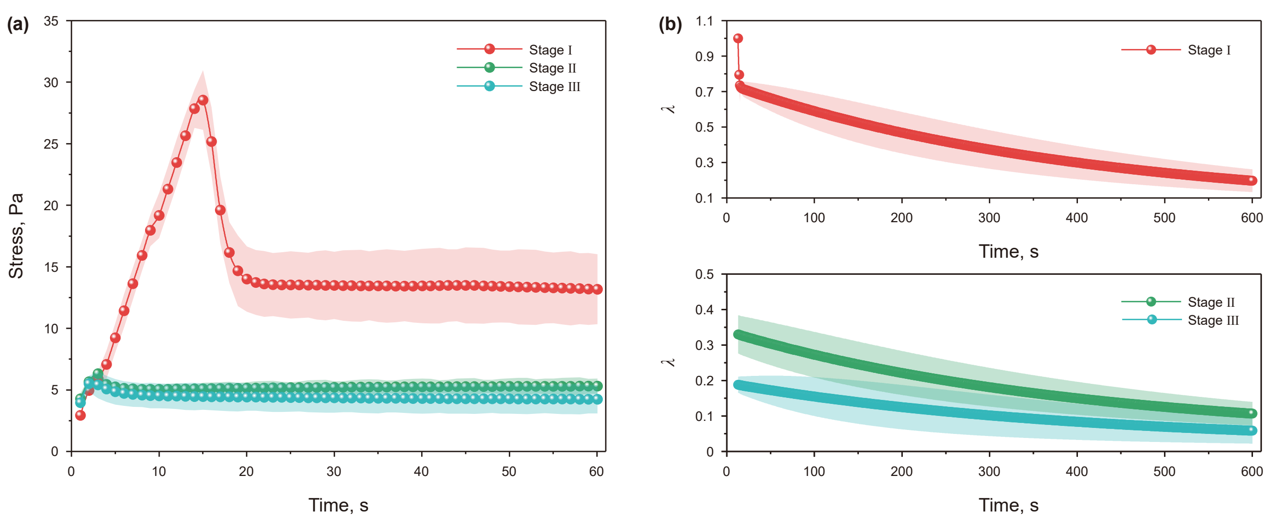

Fig. 8. Macroscopic rheological curves at different shearing stages. **(a)** Shear stress; **(b)** structural parameter. Conditions: heating temperature 60 °C; cooling rate 0.5 °C/min; shear rate 0.3 s^{-1}.

research focuses: while the reference (Cheng et al., 2000) examines how wax crystal number and area affect structural strength in systems formed during cooling, our study investigates these parameters influence post-shear. These fundamentally distinct research subjects account for the contrasting findings.

The first-stage curves in Fig. 9 demonstrate that wax crystal number, area, and fractal dimension exhibit rapid decline at the yield point, while aspect ratio shows a sharp increase. After yielding, these parameters recover and eventually reach a dynamic equilibrium state. This evolutionary pattern reveals the dynamic response mechanism of wax crystal structures under shear flow. During the rapid deformation phase of wax crystals within 1 s before yielding, the shear flow field induces both slippage and localized fracture within wax crystal aggregates. This process induces partial alignment of wax crystals under shear deformation, leading to an increased aspect ratio and reduced circularity. Simultaneously, flow-induced mutual shielding and crystal migration out of the imaging plane lead to observed reductions in crystal number and area, while increasing the average inter-crystal spacing and variance in nearest-neighbor distances. Furthermore, unidirectional shear deformation reduces morphological complexity, manifested as decreased fractal dimension. At yield onset, continued shear action causes further structural fragmentation of wax crystals, reducing aspect ratio while generating smaller crystal particles that subsequently increase number and area. Concurrently, intermolecular interactions (e.g., van der Waals forces) promote particle collision and reaggregation, with structural reconstruction rates accelerating proportionally to damage severity. Ultimately, dynamic equilibrium establishes between crystal destruction and reconstruction—mesoscopic parameters stabilize (The fluctuation amplitude between adjacent time points within a continuous 30-s period remained within ±5%) while corresponding macroscopic shear stress reaches equilibrium. Notably, macroscopic rheological data and mesoscopic parameter

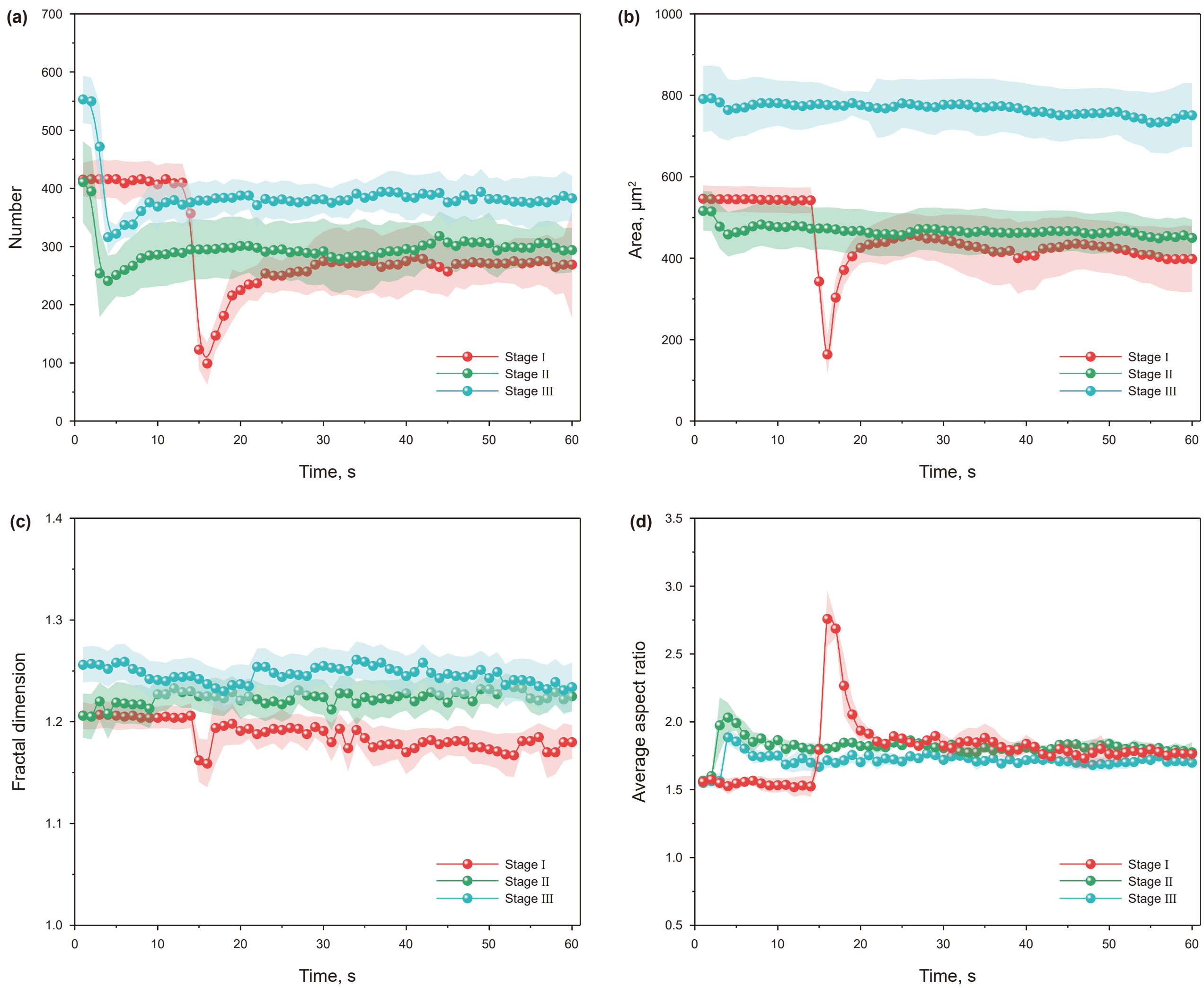

Fig. 9. Evolution curves of mesoscopic parameters for gelled waxy crude oil systems during different shear stages. **(a)** Wax crystal number; **(b)** wax crystal area; **(c)** fractal dimension; **(d)** wax crystal average aspect ratio. Conditions: heating temperature 60 °C; cooling rate 0.5 °C/min; shear rate 0.3 s^{-1}.

variations show excellent temporal synchronization (Figs. 8 and 9), confirming direct correlation between wax crystal structural evolution and bulk rheological behavior. At equilibrium state, none of the wax crystal characteristic parameters can recover to their pre-yield initial values, demonstrating that the flow field has induced irreversible modifications to the wax crystal network structure.

Comparative analysis of the three-stage shear data in Fig. 9 reveals that during the first shear stage, the variations in wax crystal mesoscopic parameters during waxy crude oil yielding exhibit significantly greater magnitudes than those observed in subsequent stages. This phenomenon occurs because initial shearing induces substantial deformation and fragmentation of large wax crystal aggregates, while the high-concentration dispersed wax crystals undergo extensive redistribution to adapt to the flow field, resulting in dramatic alterations in crystal morphology, structure, and spatial distribution. In systems that have previously experienced shearing and reached dynamic equilibrium, the wax crystal morphology, structure, and spatial distribution have already adapted to the flow field at the given shear rate. Although partial structural recovery occurs during isothermal static, reapplication of identical shear conditions produces relatively minor modifications to the wax crystal characteristics, as the system has developed structural memory of the previous shear history.

As evident from Fig. 9, increasing shear cycles lead to a rise in wax crystal number, area, and fractal dimension while reducing the aspect ratio. This phenomenon stems from progressive wax crystal fragmentation under repeated shearing, which results in more intricate spatial distribution patterns and a morphological transition toward spherical forms, consequently enhancing the crude oil's flowability. The observed microstructural evolution demonstrates that cumulative shear forces not only break down wax crystal aggregates but also modify their spatial arrangement and geometry, ultimately improving the system's rheological properties through enhanced particle dispersion and shape regularization.

3.3. *Effect of shear rate on structural breakdown and recovery characteristics of gelled waxy crude oil*

The intensity of shear action significantly impacts the structural breakdown and recovery characteristics of gelled waxy crude oil. This study conducted rheological-microscopic synchronous experiments at four different shear rates under identical thermal conditions to investigate the effects of shear rate on wax crystal morphology, structure, and spatial distribution during shear yield and isothermal recovery processes. The influence mechanism was further explored by combining macroscopic rheological curves. Fig. 10 presents the stress measurements under four shear rates at identical thermal conditions, along with structural parameter curves fitted from macroscopic experimental data using Eq. (1). To verify the consistency between the model and experimental data while ensuring model accuracy, this study applied the Hosuka model to analyze the shear stress of waxy crude oil under various shear rates. As illustrated in Fig. 10(a), the mean absolute errors ranged from 3.32% to 5.49%, with the fitted curves showing good agreement with the experimental data, demonstrating the model's ability to accurately characterize the rheological properties of crude oil under shear conditions. Comparative analysis revealed that higher shear rates resulted in shorter yield time, higher yield stress, but lower equilibrium shear stress and structural parameters. The statistical analysis of wax crystal microstructural characteristics synchronized with macroscopic rheological measurements is presented in Fig. 11. During the yielding process under four shear rates, the variations in crystal number, area, fractal dimension, and average aspect ratio within the field of view all exhibited consistent trends with those shown in Fig. 9. Comparative analysis revealed that wax crystals subjected to higher shear rates (1 s^{-1}) demonstrated the earliest changes in mesoscopic parameters, with the transition timing precisely coinciding with the yield point observed in macroscopic rheological curves. Furthermore, the magnitude of changes in mesoscopic parameters during yielding increased proportionally with loading rate. This behavior stems from the following mechanisms: Under low shear rates, only loosely arranged wax crystal flocs and weaker structural components undergo fracture and disintegration. However, as the shear rate increases, progressively fewer wax crystal structures can withstand shear-induced damage. This leads to more pronounced reductions in crystal number, area, and fractal dimension, along with increased average inter-crystal spacing and variance in nearest-neighbor distances. Concurrently, enhanced hydrodynamic drag forces induce more pronounced crystal deformation, leading to greater variations in aspect ratio and circularity (Wang et al., 2020). Moreover, higher shear rates produced increasingly significant disparities between equilibrium and initial values across all mesoscopic parameters. These findings conclusively demonstrate that external shear forces exert substantial influence on wax crystal morphology and spatial organization in waxy crude oil, with progressively more pronounced effects at greater shear intensities. Macroscopically, this manifests as shortened yield time, elevated yield stress, and diminished equilibrium shear stress and structural parameters—phenomena that fundamentally represent the shear-thinning behavior characteristic of these systems.

To investigate the mechanism of structural recovery characteristics in gelled waxy crude oil systems under different shear rates, we calculated the variation curves of structural parameters throughout the entire process (including first-stage shearing, second-stage isothermal recovery, second-stage shearing, third-stage isothermal holding, and third-stage shearing) under varying shear rates, as shown in Fig. 12. The experimental data demonstrate that when the shear rate decreases, the decline in structural parameters during the shearing stage is significantly reduced, while the recovery of structural parameters during the subsequent isothermal recovery stage is markedly enhanced. This consistent trend strongly indicates that lower shear rates are more favorable for the restoration of the wax crystal network structure.

To further elucidate the mesoscopic mechanism underlying this phenomenon, we employed microscopic observation techniques to capture the dynamic changes in mesoscopic characteristics of wax crystals during the 30-min isothermal recovery in the second stage (Fig. 13). Quantitative analysis reveals that under the same isothermal resting duration, as the pre-shear rate decreases, the growth rates of key parameters—such as wax crystal number, area, and fractal dimension—are significantly enhanced. These findings perfectly align with the structural parameter trends obtained from macroscopic rheological tests, jointly validating—from both mesoscopic and macroscopic perspectives—the influence of wax crystal reaggregation kinetics on rheological properties. This phenomenon occurs because: lower shear rates cause less damage to the wax crystal network structure, preserving more nucleation sites or skeletal frameworks that facilitate easier wax crystal reaggregation during isothermal rest, leading to higher structural recovery. Conversely, higher shear rates induce more severe destruction of the wax crystal network, resulting in stronger structural deformation and fragmentation. Consequently, the gelled system requires longer recovery periods after isothermal rest and may even exhibit incomplete recovery (Wang et al., 2020).

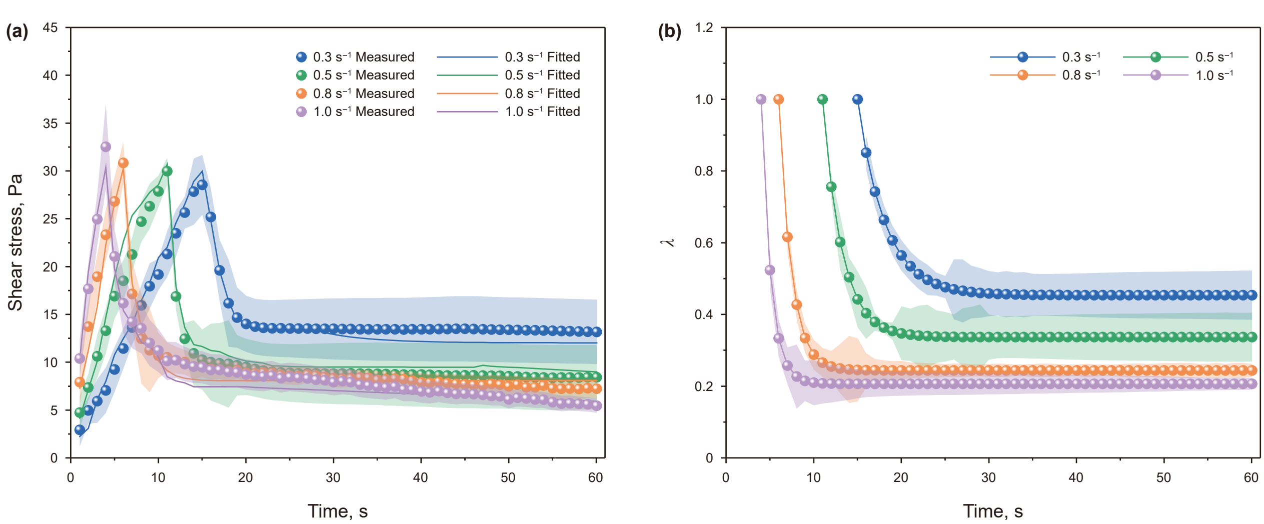

Fig. 10. Macroscopic rheological curves under different shear rates. (**a**) Shear stress; (**b**) structural parameter. Conditions: heating temperature 60 °C; cooling rate 0.5 °C/min.

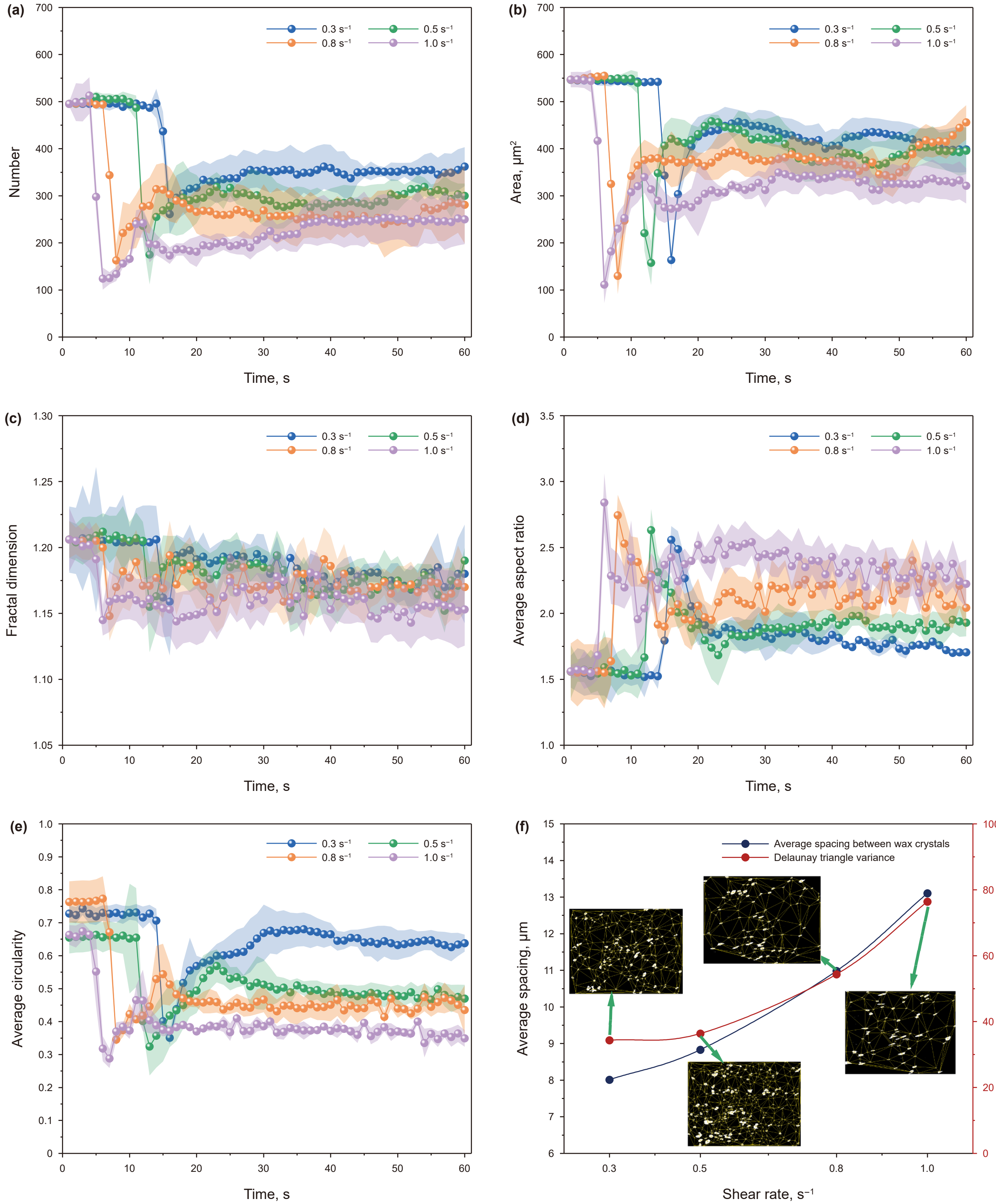

Fig. 11. Variation patterns of mesoscopic characteristics of wax crystals with shear time under different shear rates (first 60 s). **(a)** Wax crystal number; **(b)** wax crystal area; **(c)** fractal dimension; **(d)** wax crystal average aspect ratio; **(e)** wax crystal average roundness, **(f)** wax crystals spatial parameters. Conditions: heating temperature 60 °C; cooling rate 0.5 °C/min.

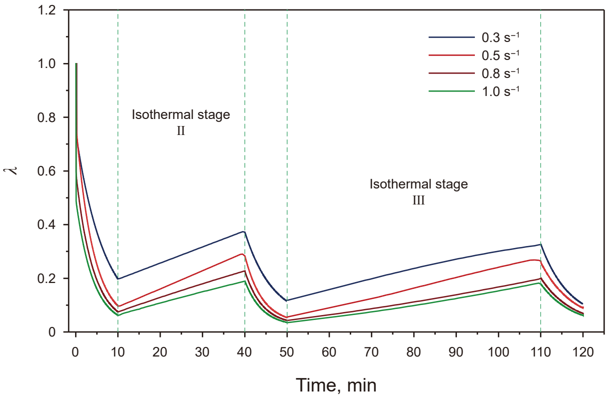

Fig. 12. Variation curves of structural parameters during shear-recovery process.

This study elucidated the wax crystal network evolution mechanism using Daqing crude oil. Future work will validate the universality by testing crude oils with diverse characteristics, and develop a generalized evolution model based on mesoscopic dynamic parameters of wax crystals, providing theoretical support for pipeline transportation across multiple oilfields.

4. Conclusions

This research utilized an integrated real-time measurement system coupling macroscopic rheological analysis with polarized microscopy to examine the dynamic evolution of wax crystal morphology during the formation, shear-induced destruction, and isothermal recovery processes of gelled crude oil's wax crystal network structure. Real-time correlation analysis with macroscopic rheological parameters yielded the following conclusions:

(1) During the first isothermal stage after cooling of waxy crude oil, initially undissolved wax crystals continuously precipitate and grow, causing significant changes in crystal number, area, fractal dimension, and average aspect ratio. As precipitation progresses, the process gradually transitions to a stage dominated by crystal growth and coalescence, where changes in mesoscopic characteristics slow down, ultimately forming the gelled structure. In contrast, during the isothermal stage after shear, only the re-adsorption and agglomeration of wax crystals occur, resulting in relatively minor changes to these characteristic parameters.

(2) During initial shearing of gelled crude oil, large wax crystals undergo deformation and fragmentation, redistributing themselves to adapt to flow field movements, leading to

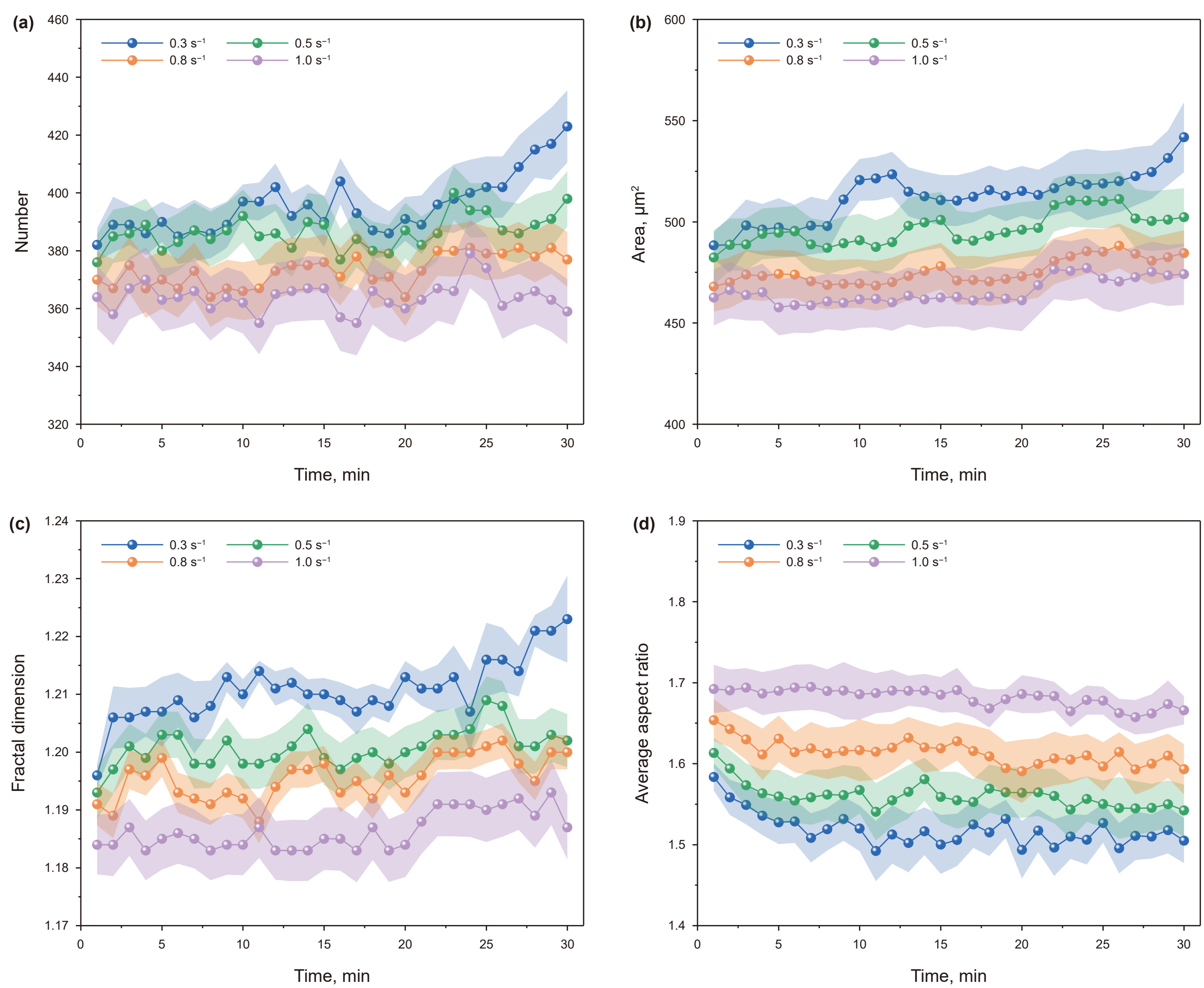

Fig. 13. Variation curves of mesoscopic characteristics of wax crystals with time during isothermal process (30 min) under different preshear rates. **(a)** Wax crystal number; **(b)** wax crystal area; **(c)** fractal dimension; **(d)** wax crystal average aspect ratio. Conditions: heating temperature 60 °C; cooling rate 0.5 °C/min.

substantial alterations in their shape, structure, and spatial distribution. Simultaneously, under van der Waals forces and other attractive interactions, wax crystals begin to collide and coalesce, with the reconstruction rate accelerating as structural damage increases. Ultimately, a dynamic equilibrium between destruction and reformation is reached. As the number of shear cycles increases, further crystal fragmentation occurs, resulting in denser and more uniform spatial distribution and increasingly spherical crystal shapes.

(3) Higher shear rates correspond to greater yield stress, shorter yield time, smaller equilibrium stress values and structural parameters in waxy crude oil, along with more irreversible damage to the wax crystal network structure and weaker static recovery capacity of the gelled structure.

The research elucidates the correlation mechanism between wax crystal mesostructure and macroscopic rheology during shear-recovery processes, explaining the fundamental nature of yield behavior, thixotropic characteristics, and shear-thinning effects through the dynamic equilibrium mechanism of wax crystal network formation, destruction, and reconstruction. This findings provides a theoretical foundation for addressing complex engineering challenges during pipeline restart operations.

CRediT authorship contribution statement

Li-Ping Guo: Conceptualization. **Jia-Jun Zhang:** Writing – original draft. **Lei Wang:** Conceptualization. **Rui Chen:** Software. **Bao-Jun Liu:** Writing – review & editing.

Declaration of competing interest

The authors declare that they have no known competing financial interests or personal relationships that could have appeared to influence the work reported in this paper.

Acknowledgements

The authors appreciate the financial support from the National Natural Science Foundation of China (No. 52574082).

References

Blake, A., Marangoni, A., 2015. The effect of shear on the microstructure and oil binding capacity of wax crystal networks. Food Biophys. 10 (4), 403–415. https://doi.org/10.1007/s11483-015-9398-z.

Bao, Y., Zhang, J., Wang, X., et al., 2016. Effect of pre-shear on structural behavior and pipeline restart of gelled waxy crude oil. RSC Adv. 6 (84), 80529–80540. https://doi.org/10.1039/c6ra16346g.

Cheng, C., Boger, D., Nguyen, Q., 2000. Influence of thermal history on the waxy structure of statically cooled waxy crude oil. SPE J. 5 (2), 148–157. https://doi.org/10.2118/57959-PA.

Dong, H., Ma, R., Zhao, J., et al., 2022. Application of rheo-optic in situ measurement technology to study waxy crude oil rheology. ACS Omega 7 (21), 17948–17962. https://doi.org/10.1021/acsomega.2c01251.

Dong, H., Zhao, J., Wei, L., et al., 2020. Effect of initial cooling temperature on structural behaviors of gelled waxy crude oil and microscopic mechanism investigation. Energy Fuel. 34 (12), 15782–15801. https://doi.org/10.1021/acs.energyfuels.0c02274.

Guo, L., Han, X., Lei, Y., et al., 2022. Research on nonlinear rheological properties of waxy crude oil based on large amplitude oscillatory shearing. J. Petrol. Sci. Eng. 213, 110444–110455. https://doi.org/10.1016/j.petrol.2022.110444.

Guo, L., Zhang, J., Sun, G., et al., 2015. Thixotropy and its estimation of water-in-waxy crude emulsion gels. J. Petrol. Sci. Eng. 131, 86–95. https://doi.org/10.1016/j.petrol.2015.04.032.

Henaut, I., Vincke, O., Brucy, F., 1999. Waxy crude oil restart: mechanical properties of gelled oils. Oil Well 349–355. https://doi.org/10.2118/56771-MS.

Hou, L., Zhang, J., 2005. An experimental study on viscoelasticity of daqing crude oil. Acta Pet. Sin. 26 (6), 109–112. https://doi.org/10.3321/j.issn:0253-2697.2005.06.025 (in Chinese).

Jia, B., Zhang, J., 2012. Yield behavior of waxy crude gel: Effect of isothermal structure development before prior applied stress. Ind. Eng. Chem. Res. 51 (33), 10977–10982. https://doi.org/10.1021/ie301047g.

Kiyingi, W., Guo, J., Xiong, R., et al., 2023. Crude oil wax: A review on formation, experimentation, prediction, and remediation techniques. Pet. Sci. 19 (5), 2343–2357. https://doi/10.1016/j.petsci.2022.08.008.

Li, H., Xie, Q., Sun, H., et al., 2022. A nonlinear creep damage model for gelled waxy crude. Pet. Sci. 19 (4), 1803–1811. https://doi/10.1016/j.petsci.2021.12.027.

Letoffe, J., Claudy, P., Kok, M., 1995. Crude oils: characterizatio of waxes precipitated on cooling by D.S.C. and thermomicroscopy. Fuel 74 (6), 810–817. https://doi.org/10.1016/0016-2361(94)00006-9.

Lin, M., Li, C., Ma, F., et al., 2009. Model and properties of isothermal gelling process for thixotropic waxy crude oil. Acta Chimica Sinica 23 (67), 2685–2691. https://doi.org/10.3321/j.issn:0567-7351.2009.23.007 (in Chinese).

Li, C., Lu, Q., 2004. Research on irreversible thixotropy and its mechanisms in non-newtonian crude oils, pp. 19–21. https://doi.org/10.3969/j.issn.1006-6896.2004.11.011, 23 (11) (in Chinese).

Mohammadi, S., Mahmoudi, A., 2021. Simultaneous control of formation and growth of asphaltene solids and wax crystals using single-walled carbon nanotubes: an experimental study under real oilfield conditions. Energy Fuel. 35 (18), 14709–14724. https://doi/full/10.1021/acs.energyfuels.1c02244.

Srivastava, S., Butz, T., Verma, P., 2002. Study of the temperature and enthalpy of wax crystallization from middle distillate by DSC. Petrol. Sci. Technol. 20, 831–839. https://doi.org/10.1081/LFT-120003716.

Shuang, K., Liang, Q., Zhang, J., 2002. Quantitative characterization of wax crystal morphology in waxy crudes. J. China Univ. Petrol. (Nat. Sci. Ed.) 26 (5), 101–103. https://doi.org/10.3969/j.issn.2096-1693.2017.02.024 (in Chinese).

Sun, G., Li, C., Yang, S., et al., 2019. Experimental investigation of the rheological properties of a typical waxy crude oil treated with supercritical CO_2 and the stability change in its emulsion. Energy Fuel. 33, 4731–4739. https://doi.org/10.1021/acs.energyfuels.8b04176.

Teng, H., Zhang, J., 2013. A new thixotropic model for waxy crude. Rheol. Acta 52 (10–12), 903–911. https://doi.org/10.1007/s00397-013-0729-z.

Venkatesan, R., Nagarajan, N., Paso, K., et al., 2005. The strength of paraffin gels formed Tinder static and flow conditions. Chem. Eng. Sci. 60 (13), 3587–3598. https://doi.org/10.1016/j.ces.2005.02.045.

Wang, Z., Li, S., Jin, Z., et al., 2023. Oil and gas pathway to net-zero: review and outlook. Energy Strategy Rev. 45, 101048. https://doi/101048.10.1016/j.esr.2022.101048.

Wang, Z., Wang, H., Zhu, C., et al., 2020. A novel method for characterizing the aggregation of wax crystals and an improvement in wax deposition model. J. Energy Resour. Technol. 142 (10), 103003–103015. https://doi.org/10.1115/1.4047083.

Yao, B., Zhu, H., Yan, B., et al., 2023. Pre-heating temperature induced flowability and wax deposition characteristics of crude oil adding wax inhibitors. Pet. Sci. 20 (4), 2468–2478. https://doi/10.1016/j.petsci.2023.02.030.

Zhao, J., Xi, X., Dong, H., et al., 2021. In-situ observation of microscopic motions and structure dynamic transformation of wax crystals in waxy crude oil subjected to shear. New J. Chem. 45 (37), 17522–17543. https://doi.org/10.1039/d1nj02292j.

Zhao, J., Zhuo, Z., Dong, H., et al., 2024. Structural failure process of gelled waxy crude oil emulsion based on rheological-in-situ microscopic synchronous measurement. Fuel 364, 131070–131085. https://doi.org/10.1016/j.fuel.2024.131070.